Olefin Epoxidation with Transition Metal η^2-Peroxo Complexes: The Control of Reactivity

Dirk V. Deubel,*[a,b] Jörg Sundermeyer,[a] and Gernot Frenking*[a]

Keywords: Density functional calculations / Epoxidations / Peroxo complexes / Transition states

The activation energies for olefin epoxidation with Mimoun-type η^2-peroxo complexes have been calculated using density functional methods. Six degrees of freedom of the complex [MOL$(O_2)$$(OER_3)$] and the olefin CH_2CHR' have been systematically modified. The calculations were based on the assumptions that the reaction follows a concerted oxygen-transfer mechanism suggested by Sharpless and that a peroxo oxygen atom *trans* to the phosphane oxide ligand is transferred. This was recently proved for the epoxidation of ethylene with the parent complex [$MoO(O_2)_2${$OP(CH_3)_3$}]. It has been found that the diperoxotungsten complexes (M = W; L = O_2) are more reactive than the diperoxomolybdenum complexes (M = Mo; L = O_2). The activation barriers for the monoperoxomolybdenum complexes (M = Mo; L = O) are significantly higher than the barriers for the corresponding diperoxo complexes (M = Mo; L = O_2), whereas equal activation energies have been predicted for both tungsten compounds (M = W; L = O_2 and O). The influence of the pnicogen oxide OER_3 on epoxidation activity is comparably small, while electron-releasing substituents R′ at the C=C bond reduce the activation barrier. The transition states for the epoxidation of alkenes with conjugated double bonds show a large extent of asymmetry, with the C–O bond at the terminal carbon atom being formed first. Additional ligands L′ coordinating to the metal center inhibit oxygen transfer. The results are in agreement with an electrophilic attack of the oxidant on the C=C double bond.

Introduction

Tremendous research efforts have focused on the epoxidation of olefins mediated by transition metal complexes,[1−7] in order to replace the chlorohydrin process which is still utilized on a million-ton-per-year scale despite its inefficiency and environmental impact.[8] Beside Herrmann-type diperoxorhenium compounds,[6] Mimoun-type diperoxo complexes of group 6 metals have been utilized as oxidants for olefins. As a promising method based on the *stoichiometric* epoxidation with Mimoun-type diperoxomolybdenum complexes [$MoO(O_2)_2(OPR_3)$] (R = NMe_2),[9] a *biphasic catalytic* system (R = *n*-dodecyl) has recently been developed[10] and patented by BASF.[11] Furthermore, *catalytic* methods in *one homogeneous phase* involving oxo- and diperoxomolybdenum compounds with the hmpa ligand (R = NMe_2)[12] and the 3-pyrazolylpyridine-*N*,*N*′ ligand[13] were reported.

In the last decade, modern computational chemistry has become an important tool in clarifying mechanisms of metal-complex-mediated epoxidations.[14−21] The long-standing controversy[22] about the mechanism of olefin epoxidation with Mimoun-type η^2-diperoxomolybdenum complexes [$MoO(O_2)_2(OPR_3)$] (**I**) has recently been settled with the help of density functional methods (Scheme 1).[16] The reaction does not follow a step-wise pathway[23] involving olefin coordination at the metal center (**II**), subsequent cycloinsertion yielding a 2,3-metalladioxolane (**III**), and cycloextrusion of the oxirane (**IV**) from the metallacycle. Although olefins coordinate with the d^0 metal center of the diperoxomolybdenum complexes (**I→II**),[24] subsequent formation of the metalladioxolane (**II→III**) does not occur; nor is a direct reaction pathway (**I→III**) from the reactants to the metallacycle energetically feasible.[16] Even if the metallacycle was formed, its decomposition would yield the carbonyl compound (**VI**) via hydrogen-migration-supported cycloreversion, rather than the epoxide (**IV**) via cycloextrusion (Scheme 2).[16] As suggested by Sharpless,[25] the oxygen atom is directly transferred from the metal peroxide to the olefin (**TS V**). Preferentially, the peroxo oxygen atom *trans*[26] to the phosphane oxide ligand is transferred and it has a *spiro* configuration in the **TS** geometry.[16] The transition state shows an anomeric effect, i.e. the O−P bond of the phosphane oxide is synperiplanar to the metal−oxygen bond being cleaved.[16,24] The concerted mechanism was also proved for olefin epoxidation with the methyloxodiperoxorhenium(VII) compound.[14] The electronic character of the oxygen transfer was clarified by Charge Decomposition Analysis (CDA)[27] of **TS V**.[20] The analysis identified donation *d* from the ethylene HOMO into the σ* orbital of the O−O bond as the predominant interaction (Figure 1). Backdonation *b*, from the oxygen lone pairs into the ethylene LUMO is significantly less important. This indicates an electrophilic attack of the metal peroxide on the olefin.[20]

Since the activation energy for the epoxidation of ethylene with [$MoO(O_2)_2${$OP(CH_3)_3$}] was calculated to be comparably high (18 kcal/mol),[16] the objective of this DFT study was to investigate the control of reactivity. A general-

[a] Fachbereich Chemie, Philipps-Universität Marburg, Hans-Meerwein-Straße, 35032 Marburg, Germany
[b] Department of Chemistry, University of Calgary, 2500 University Drive N. W., Calgary, Alberta T2N 1N4, Canada

  1434−1948/01/0707−1819 $ 17.50+.50/0

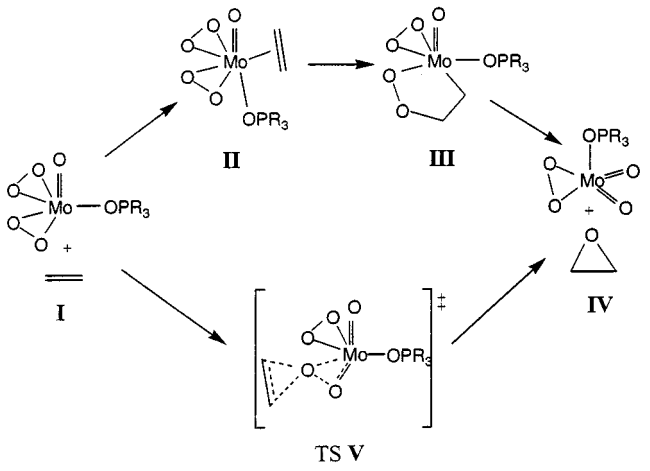

Scheme 1. The long-standing controversy about the mechanism of olefin epoxidation with Mimoun-type diperoxo complexes; the reaction follows a concerted pathway via **TS V**

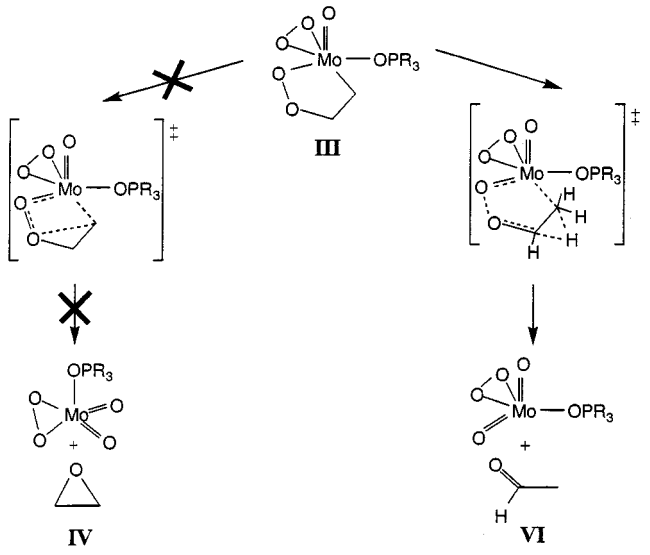

Scheme 2. Fragmentation of the metallacycle; hydrogen-migration-supported cycloreversion (**III→VI**) is favored over the cycloextrusion of oxirane (**III→IV**)

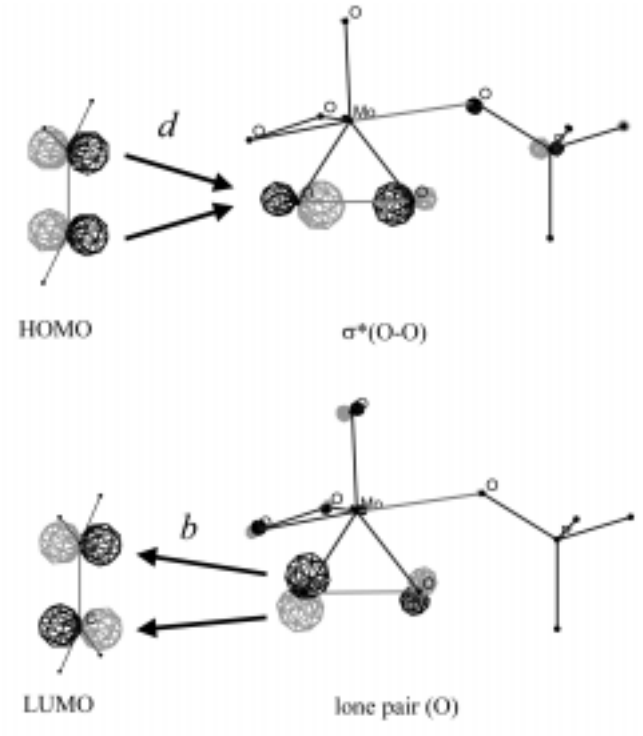

Figure 1. Predominant orbital interactions in the transition state for the epoxidation of ethylene with $[MoO(O_2)_2(OPH_3)]$; donation *d* is significantly more important than backdonation *b*

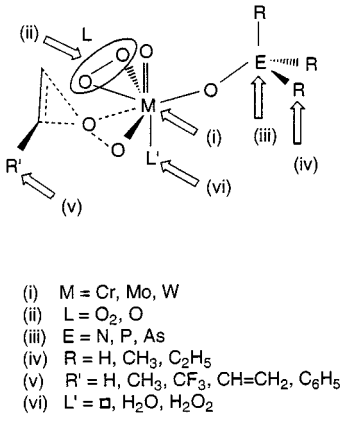

Scheme 3. Concepts for the control of reactivity of olefin oxidation with Mimoun-type peroxo complexes

ized model consisting of the metal complex $[MOL(O)_2(OER_3)L']$ and a terminal olefin CH_2CHR', contains six reactivity-determining degrees of freedom (Scheme 3) which are systematically modified in this study: (i) the metal center M, (ii) the oxo or peroxo ligand L, (iii) pnicogen E, (iv) the substituents R at the pnicogen atom, (v) the substituent R′ at the olefin, and (vi) additional ligands L′ at the metal center. The calculations were based on the assumption that the reaction follows the same concerted pathway as ethylene epoxidation with the parent complex $[MoO(O_2)_2\{OP(CH_3)_3\}]$.[16] Note that, in the catalytic systems, the coordination of the oxidant such as hydrogen peroxide, silyl peroxides, or *tert*-butyl hydroperoxide to the metal center and subsequent proton transfer can yield different species which are potentially more reactive than the parent η^2-peroxo complex.[10,13,17,21] Unless otherwise stated, transfer of the peroxo oxygen atom, which is located *trans* to the phosphane oxide, has been considered.[26]

Methods

The geometries of the molecules and transition states (**TS**) were optimized using the 3-parameter fit of the exchange potentials introduced by Becke (B3LYP).[28] Relativistic small-core ECPs[29] with a valence basis set splitting (441/2111/N1) were used for Cr (N = 4), Mo (N = 3), and W (N = 2), while 6−31G(d) all-electron basis sets were employed for the other atoms.[30] This is our standard basis set

II.[31] Vibrational frequencies and zero-point energy contributions (ZPE) were also calculated at B3LYP/II. All structures reported here are either minima (NIMAG = 0) or transition states (NIMAG = 1, **TS**) on the potential energy surface. The ZPE corrections are unscaled. Improved total energies were calculated at the B3LYP level using the same ECP and valence basis set for the metal atom, but totally uncontracted and augmented with one set of f-type polarization functions,[32] together with 6−31+G(d) basis sets for the other atoms.[33] This basis set combination is denoted III+.[34] Unless otherwise stated, the energies reported refer to the B3LYP/III+//B3LYP/II level of theory. For selected molecules, NPA atomic partial charges were calculated.[35] The computations were carried out with the program package Gaussian 98.[36]

Donor−acceptor interactions in selected transition states were examined using Charge Decomposition Analysis (CDA),[27] which is a quantitative interpretation of the Dewar−Chatt−Duncanson model.[37] The Kohn−Sham orbitals of the **TS** are expressed as a linear combination of the orbitals of the olefin and the remaining metal fragment [M] in the **TS** geometry. The orbital contributions are divided into the mixing of the occupied MOs of the olefin and the vacant orbitals of [M] (donation *d* $C_2H_3R'\rightarrow$[M]), the mixing of the vacant MOs of the olefin and the occupied orbitals of [M] (backdonation *b* $C_2H_3R'\leftarrow$[M]), and the mixing of the occupied MOs of the olefin and the occupied orbitals of [M] (repulsive polarization *r* $C_2H_3R'\rightleftarrows$[M]). A fourth term denoted as the rest term Δ gives the mixing of the unoccupied MOs of the olefin and the unoccupied MOs of [M]. The Δ term will be approximately zero if a discussion of the **TS** in terms of donor−acceptor interactions is permissible. The CDA calculations were performed using the program CDA 2.1.[38]

Results and Discussion

Tables 1−7 list the calculated activation energies for 21 systematically selected combinations (i−vi). In the tables and figures, reactants are denoted **R** and transition states are denoted **TS**. For the coordination of additional ligands L′ at the metal center (vi), stabilization energies were also calculated. The stabilized complexes are denoted **C**. The activation energies given in Table 7 refer to the stabilized complexes **C**.

(i) Influence of the Metal M

Since the patents of BASF[11] include the Mimoun-type diperoxotungsten complexes in addition to the molybdenum compounds, we are extending our study to all the group 6 metals. The reactivity of the diperoxo complexes $[MO(O_2)_2(OPR_3)]$, with M = Cr, Mo, W, with respect to ethylene epoxidation can easily be predicted. Since the oxidant attacks the olefin in an electrophilic manner,[16] the partial charges at the peroxy oxygen atoms of the free oxidants should be a measure of epoxidation activity. NPA partial charges of the three metal diperoxides are shown in Figure 2.[35] At the metal center, the charges increase from chromium to tungsten. Negative charges at the peroxo oxygen atoms of $[MO(O_2)_2(OPR_3)]$ increase in the same order; the highly negatively charged oxygen atoms of the tungsten complex are less electrophilic, and this complex should therefore be less reactive. This conclusion is supported by the reaction energies; according to the Bell−Evans−Polanyi principle,[39] a lower barrier for the chromium complex is expected due to the more exothermic reaction (Table 1). These results suggest that the activation energies increase in the order Cr < Mo < W.

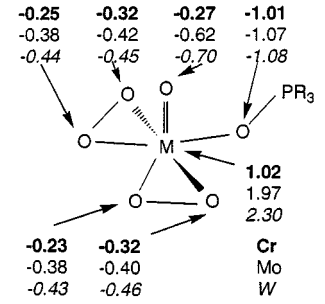

Figure 2. Calculated NPA partial charges of $[MO(O_2)_2\{OP(CH_3)_3\}]$; M = Cr (**R 1**, **bold**), Mo (**R 2**, plain), W (**R 3**, *italics*)

Table 1. O−O distances [Å] in diperoxo complexes $[MO(O_2)_2\{OP(CH_3)_3\}]$; M = Cr (**1**), Mo (**2**), W (**3**), *d*/*b* ratio in CDA of the transition states of ethylene epoxidation, reaction energies E_r [kcal/mol] and activation energies E_a [kcal/mol]; energies at the B3LYP/III+//B3LYP/II level; ZPE-corrected (B3LYP/II) values in parentheses

No.[a]	M	O−O	*d*/*b*	E_r	E_a
1	Cr	1.404	1.63[b]	−42.5 (−40.1)	21.8 (23.1)
2	Mo	1.452	1.76[c]	−37.2 (−35.4)	16.9 (17.9)
3	W	1.478	1.86[d]	−36.9 (−35.0)	14.5 (15.4)

[a] For geometry optimizations and frequency calculations, basis set STO-3G was used at the methyl groups. − [b] $d = 0.237$, $b = 0.145$, $r = -0.318$, $\Delta = -0.005$. − [c] $d = 0.237$, $b = 0.135$, $r = -0.312$, $\Delta = -0.004$. − [d] $d = 0.233$, $b = 0.125$, $r = -0.301$, $\Delta = -0.005$.

However, the calculated activation barriers show the opposite trend. Activation energies for ethylene epoxidation with $[MO(O_2)_2\{OP(CH_3)_3\}]$ decrease from chromium (23.1 kcal/mol), molybdenum (17.9 kcal/mol) to tungsten (15.4 kcal/mol, Table 1). Rösch and co-workers[19] have recently studied the epoxidation of ethylene with simpler model complexes $[MO(O_2)_2(NH_3)]$ using DFT methods. They found a similar trend for the activation energies with M = Cr, Mo, W.[40] A correlation between the σ*-orbital energy level and the activation barrier was given as an explanation.[18] This is plausible because donation from the olefin HOMO into the σ* orbital of the O−O bond being cleaved is the dominant interaction in the **TS**.[20] Furthermore, Rösch and co-workers[19] pointed out a stronger involvement of the metal d orbitals in the π* orbital of the O−O bond in the chromium compound, which increases the strength of the O−O bond and lowers the epoxidation ac-

tivity. This is also reflected by the O−O distances in the free oxidants (Table 1).

Originally, a three-membered ring transition state shown in Figure 3a was suggested.[25] If this had been true, the partial charges of the metal complexes would have led to the correct prediction of the epoxidation activity. We want to point out that the transition state is coarctate,[41] i.e. the metalladioxirane moiety is significantly involved, as schematically shown in Figure 3b. Therefore, the sum of partial charges $q(M) + q(O) + q(O)$ at the metalladioxirane moiety (Figure 2) predicts the trend of the activation barriers in relation to an electrophilic attack. A fragment-based population analysis, such as Charge Decomposition Analysis (CDA),[27] should also reflect the trend; the CDA results of the transition states are given in Table 1. The ratio donation/backdonation (d/b) is a measure of the electronic character of the oxidants. The analysis reveals that the d/b values, and therefore the electrophilicity of the oxidants increase in the order Cr < Mo < W. Since the oxidant attacks the olefin in an electrophilic manner, the reactivity of comparable oxygen-transfer agents correlates with their electrophilicity.

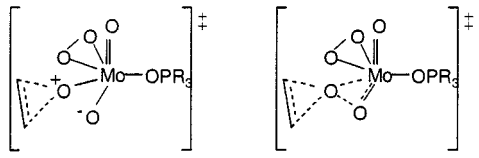

Figure 3. The nature of the transition state for olefin epoxidation with transition metal peroxo complexes: a) **TS** involving only the olefin and the oxygen atom that is transferred, b) coarctate **TS**

(ii) Reactivity of Monoperoxo Complexes

Olefin epoxidation with a diperoxo complex yields the oxirane2 and the monoperoxo complex, which might then oxidize an olefin. To highlight the reactivity of the monoperoxomolybdenum compounds, we calculated the activation energies for the epoxidation of ethylene with $[MoO(O_2)L(OPR_3)]$ (L = O_2, O; Table 2). CDA results are also given in Table 2. In contrast to the transition states presented in the other sections, both isomers of the **TS**s, i.e. for an olefin attack at the peroxo oxygen atom *cis* and *trans* to the phosphane oxide, have been considered since the preferential attack has not yet been clarified for the monoperoxo complexes. The **TS**s for a *cis* attack are denoted **c**. Figure 4 shows the optimized structures for the transition states of ethylene epoxidation with the molybdenum diperoxides $[MoO(O_2)_2(OPH_3)]$ (**TS 10** and **TS 10c**, respectively) and monoperoxides $[MoO_2(O_2)(OPH_3)]$ (**TS 12** and **TS 12c**, respectively). CDA of the diperoxo compounds indicates that the transfer of the *cis* oxygen atom is less electrophilic (**TS 10c**: $d/b = 1.60$), and therefore less reactive (E_a = 24.7 kcal/mol) than the transfer of the *trans* oxygen atom (**TS 10**: $d/b = 1.92$, E_a = 15.2 kcal/mol). The corresponding results for the monoperoxo complexes are surprising. Although the peroxo oxygen atom situated *trans* is also more electrophilic ($d/b = 2.00$ for **TS 12** versus 1.68 for **TS 12c**), the activation barriers are almost equal (17.8 and 18.0 kcal/mol, respectively). Does our simple model fail to explain the reactivity of the monoperoxo complexes? Note the optimized structures of the reactants given in Figure 5. While $[MoO(O_2)_2(OPR_3)]$ (**R 10**) has Mo−O(peroxo) bonds of equal length, the Mo−O(peroxo) bonds situated *cis* to the phosphane oxide in $[MoO_2(O_2)(OPR_3)]$ (**R 12**) are elongated. The cleavage of these bonds is already reflected by the reactant geometry, which is the reason for a moderate barrier despite its lower electrophilicity. CDA apparently describes the nature of the O−O bond rather than the metal−O(peroxo) bond. Bach and co-workers[42] pointed out for other oxidants that a prediction of activation energies based only on parameters of the O−O bond being cleaved is not always successful. In metal peroxides, the strength of the M−O bonds, reflected by their length, also has to be taken into account.

Table 2. Calculated (B3LYP/III+//B3LYP/II) activation energies E_a [kcal/mol] and CDA results of transition states of ethylene epoxidation with the diperoxo and monoperoxo complex $[MoOL(O_2)(OPH_3)]$; L = O_2 (**R 10**), O (**R 12**)

TS[a]	d $C_2H_4\rightarrow$[M]	b $C_2H_4\leftarrow$[M]	d/b	r $C_2H_4\leftrightarrow$[M]	Δ	E_a
TS 10	0.223	0.116	1.92	−0.275	−0.005	14.2 (15.2)
TS 10c	0.230	0.144	1.60	−0.332	−0.005	23.8 (24.7)
TS 12	0.230	0.115	2.00	−0.288	−0.004	17.0 (17.8)
TS 12c	0.208	0.124	1.68	−0.283	−0.005	17.0 (18.0)

[a] **TS** for an olefin attack on the peroxo oxygen atom *cis* to the phosphane oxide ligand are denoted **c**. Otherwise, the *trans* peroxo atom is attacked.

Olefin epoxidation with several (monoperoxo)Mo^{VI} complexes of the type $[X_2MoO(O_2)(H_2O)(NH_3)]$ was recently studied by Rösch and co-workers using density functional methods.[18] These monoperoxo complexes exhibit higher barriers for direct oxygen transfer to ethylene than those for the reference diperoxo complex $[MoO(O_2)_2(H_2O)(NH_3)]$.[18] The most electronegative ligands X induce the lowest barriers, which is in agreement with the concept of an electrophilic attack of the molybdenum peroxide on the olefin.

Our calculations reveal that the monoperoxomolybdenum complexes (**R 12**: E_a = 17.8 kcal/mol) are less reactive than the diperoxo complexes (**R 10**: E_a = 15.2 kcal/mol). The small reactivity of monoperoxomolybdenum compounds was supported by experiments[10,43] and a recent theoretical[18] study. However, the data provided in Table 3 reveal that the reactivities of the tungsten compounds are different. The calculated activation barriers for ethylene epoxidation with the monoperoxo- (**R 13**: E_a = 13.5 kcal/mol) and diperoxotungsten compounds (**R 11**: E_a = 12.7 kcal/mol) are almost equal, indicating that both tungsten species are active oxidants.

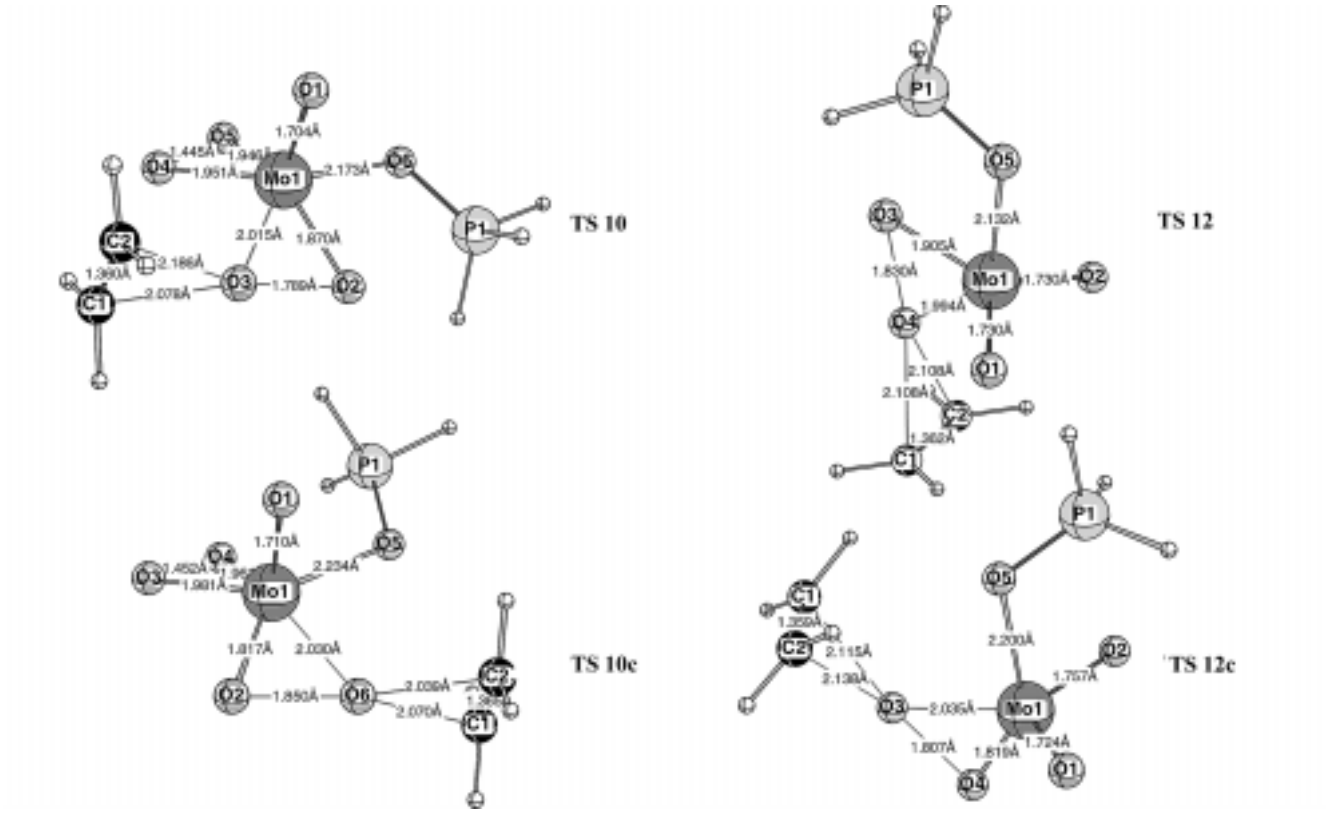

Figure 4. Optimized geometry of **TS 10**, **TS 10c**, **TS 12**, and **TS 12c** (B3LYP/II)

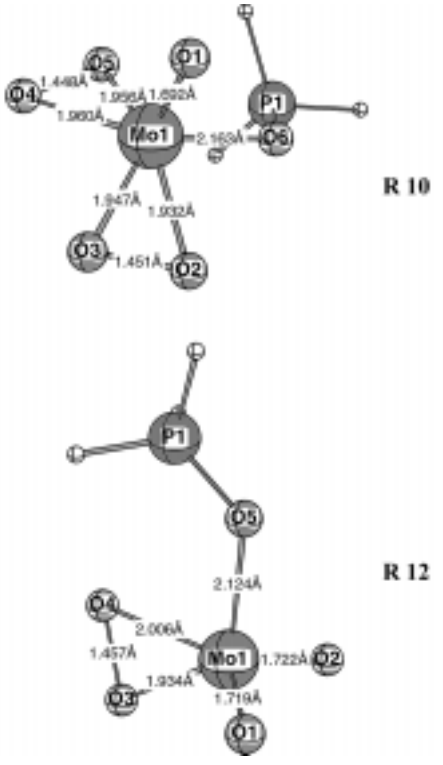

Figure 5. Optimized geometry of **R 10** and **R 12** (B3LYP/II)

(iii) Influence of the Pnicogen E

Besides amphiphilic phosphane oxide ligands, the corresponding amine and arsane oxides are used in the metal-catalyzed epoxidation under biphasic conditions.[10,11] Thus, we have investigated the reactivity of the diperoxo complexes $[MO(O_2)_2\{OE(CH_3)_3\}]$ with M = Cr, Mo, W and with E = N, P, As. The results given in Table 4 are similar for the three metals; we focus on the molybdenum compounds for which the largest differences in the activation barriers are found. The calculations show that the complexes with the phosphane oxide ligands tend to be slightly more reactive than the amine and arsane oxide complexes. Phosphane oxides are weaker donors than their N and As analogues. Therefore, the OPR_3 complexes are more electrophilic at the metalladioxirane moieties and more reactive. This is in agreement with the experimental results for stoichiometric olefin epoxidation.[10] Surprisingly, the opposite trend is found for the reaction performed under biphasic conditions. In this system, the phosphane oxide complexes are less efficient.[10] Note that the turnover frequencies depend both on the intrinsic reactivity of the oxidants and on their Nernst distribution in the two phases. Amine and arsane oxides are comparably strong donors and they can extract the catalyst more efficiently into the organic phase, where epoxidation occurs. Despite higher activation barriers, the E = N, As systems are better oxidants under biphasic conditions due to their better extracting abilities,

which leads to a larger concentration of catalyst in the organic phase.[10] Although one should not over-interpret the small calculated differences in activation energies, the theoretically predicted activation barriers reflect the experimental trends.

Table 3. Calculated (B3LYP/III+//B3LYP/II) activation energies E_a [kcal/mol] for ethylene epoxidation with mono- and diperoxo complexes [$MOL(O_2)\{OE(CH_3)_3\}$]; M = Mo, W; L = O_2, O; ZPE-corrected (B3LYP/II) values are given in parentheses

No.[a]	(i) M	(ii) L	(iii) E	(iv) R	(v) R′	(vi) L′	E_a
10	Mo	O_2	P	H	H	□	14.2 (15.2)
10c	Mo	O_2	P	H	H	□	23.8 (24.7)
11	W	O_2	P	H	H	□	11.9 (12.7)
12	Mo	O	P	H	H	□	17.0 (17.8)
12c	Mo	O	P	H	H	□	17.0 (18.0)
13	W	O	P	H	H	□	12.7 (13.5)
13c	W	O	P	H	H	□	13.4 (14.4)

[a] **TS** for an olefin attack on the peroxo oxygen atom *cis* to the phosphane oxide ligand are denoted **c**. Otherwise, the *trans* peroxo oxygen is attacked. – [b] □ = free coordination site.

Table 4. Calculated (B3LYP/III+//B3LYP/II) activation energies E_a [kcal/mol] for ethylene epoxidation with diperoxo complexes [$MO(O_2)_2\{OE(CH_3)_3\}$]; M = Cr, Mo, W; E = N, P, As; ZPE-corrected (B3LYP/II) values are given in parentheses

No.	(i) M	(ii) L	(iii) E	(iv) R[a]	(v) R′	(vi) L′	E_a
1	Cr	O_2	P	CH_3	H		21.8 (23.1)
2	Mo	O_2	P	CH_3	H		16.9 (17.9)
3	W	O_2	P	CH_3	H		14.5 (15.4)
4	Cr	O_2	N	CH_3	H		22.3 (23.3)
5	Mo	O_2	N	CH_3	H		17.8 (18.7)
6	W	O_2	N	CH_3	H		15.1 (16.0)
7	Cr	O_2	As	CH_3	H		22.0 (22.9)
8	Mo	O_2	As	CH_3	H		18.6 (19.6)
9	W	O_2	As	CH_3	H		14.4 (15.3)

[a] For geometry optimizations and frequency calculations, basis set STO-3G was used at the methyl groups. – [b] □ = free coordination site.

(iv) Influence of Substituents R at the Pnicogen Oxide

Amphiphilic pnicogen oxides with long alkyl chains *n*-C_kH_{2k+1} are used as ligands in the biphasic system. The turnover frequencies strongly depend on the chain length *k*; after increasing with increasing *k*, they remain constant from about $k = 8$.[32] The crucial question is whether the chain length has an influence on the reactivity of the complex, or only on its Nernst distribution equilibrium. Thus, we calculated activation energies for the epoxidation of ethylene by [$MoO(O_2)_2(OPR_3)$] with R = H, CH_3, C_2H_5 (Table 5). The decreasing reactivity from the phosphane oxide complexes (R = H, E_a = 15.2 kcal/mol) to the trimethylphosphane oxide complexes (R = CH_3, E_a = 17.5 kcal/mol) arises from a larger electron density at the metal center and at the peroxo oxygen atoms in the latter compound. The important result for the complex with R = C_2H_5 should be noted. The activation barrier increases by only 0.4 kcal/mol compared with that for the complex with R = CH_3. Alkyl chains longer than $k = 1$ influence the concentration of the catalyst [$MoO(O_2)_2\{OP(n\text{-}C_kH_{2k+1})_3\}$] in the organic phase rather than the reactivity. Therefore, trimethylphosphane oxide is an excellent model for the amphiphilic ligand in computational studies on the control of reactivity.[45]

Table 5. Calculated (B3LYP/III+//B3LYP/II) activation energies E_a [kcal/mol] for ethylene epoxidation with [$MoO(O_2)_2(OPR_3)$]; R = H, CH_3, C_2H_5; ZPE-corrected (B3LYP/II) values are given in parentheses

No.	(i) M	(ii) L	(iii) E	(iv) R	(v) R′	(vi) L′	E_a
10	Mo	O_2	P	H	H	□	14.2 (15.2)
2	Mo	O_2	P	CH_3 [a]	H	□	16.9 (17.9)
14	Mo	O_2	P	CH_3	H	□	16.6 (17.5)
15	Mo	O_2	P	C_2H_5	H	□	17.1 (17.9)

[a] For geometry optimizations and frequency calculations, basis set STO-3G was used at the methyl groups.

(v) Influence of Substituents R′ at the Olefin

In our quantum-chemical calculations, ethylene has been used as a model for the olefin, although the homogeneously catalytic activation of hydrogen peroxide is probably unnecessary for the industrial production of ethylene oxide. Heterogeneously catalytic epoxidation on silver surfaces with O_2 as the oxidant works perfectly for ethylene, but fails for alkyl-substituted olefins due to a chemoselectivity problem. Allylic C–H bonds of the latter substrates are preferentially oxidized.[46] Thus, we are expanding our study of epoxidation with [$MoO(O_2)_2(OPH_3)$] to olefins of the type C_2H_3R', with a variety of substituents R′ = H, CH_3, CF_3, $CH{=}CH_2$, C_6H_5. Since attempts to induce an enantioface selectivity of olefin epoxidation by the employment of chiral phosphane oxide ligands failed,[44] only one of four diastereomeric transition states was arbitrarily selected for the attack at the peroxo oxygen atom *trans* to the OPR_3 ligand, and was optimized with all substituents R′ (Scheme 3). Electron-donating substituents might lower the barrier and vice versa, because donation from the olefin HOMO into the σ*(O–O) orbital is the predominant interaction in the transition state. The data given in Table 6 confirm this hypothesis. The calculated barrier for 3,3,3-trifluoropropene (17.2 kcal/mol) is higher than for ethylene (15.2 kcal/mol), whereas propylene is oxidized faster (E_a = 12.9 kcal/mol). Additional alkyl substituents at the olefin should further accelerate the reaction.[23] π-Conjugation in *transoid*-butadiene and styrene also leads to slightly smaller activation barriers. While the orbital coefficients at the carbon atoms in the olefin HOMO decrease, the energy of this orbital increases due to conjugation.[47] The geometry of **TS 18** for *transoid*-butadiene given in Figure 6 reveals a strongly asynchronous but still concerted epoxidation of conjugated double bonds. The C–O bond at the terminal carbon atom

Table 6. Calculated (B3LYP/III+//B3LYP/II) activation energies E_a [kcal/mol] for epoxidation of olefins CH_2=CHR, R′ = H, CF_3, CH_3, CH=CH_2, C_6H_5 with [$MoO(O_2)_2(OPH_3)$]; ZPE-corrected (B3LYP/II) values are given in parentheses

No.	(i) M	(ii) L	(iii) E	(iv) R	(v) R′	(vi) L′	E_a
10	Mo	O_2	P	H	H	□	14.2 (15.2)
16	Mo	O_2	P	H	CF_3	□	16.9 (17.2)
17	Mo	O_2	P	H	CH_3	□	12.4 (12.9)
18	Mo	O_2	P	H	CH=CH_2	□	12.6 (7.4)
19	Mo	O_2	P	H	C_6H_5	□	12.0 (12.5)

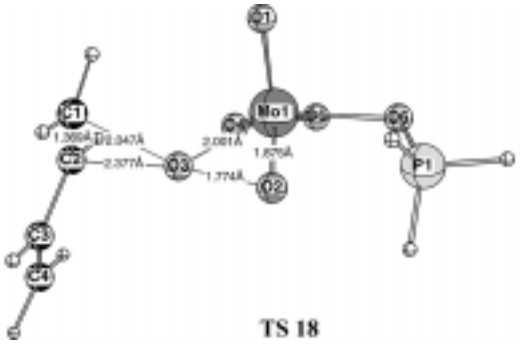

Figure 6. Optimized geometry of **TS 18** (B3LYP/II)

C1 is formed first because of the larger coefficient at C1 in the olefin HOMO.[47]

(vi) Influence of Additional Ligands L′ at the Metal Center

Due to the solubility of hydrogen peroxide in the organic phase ($CHCl_3$), epoxidation can occur in a different manner than that has been discussed for homogeneous *t*BuOOH activation:[13] Hydrogen peroxide can coordinate at the metal center, and catalytically active species might be formed in subsequent reactions.[13] In this section, we investigate the influence of an additional ligand L′ = H_2O, H_2O_2 on the stability and reactivity of diperoxo complexes [$MoO(O_2)_2(OPR_3)L'$]. The results are collected in Table 7. The coordination of an aqua and hydrogen peroxide ligand to [$MoO(O_2)_2\{OP(CH_3)_3\}$] is exothermic by −8.6 and −12.6 kcal/mol, respectively.[48,49] However, in agreement with the electrophilicity concept, the additional ligand increases the electron density at the reactive site and should therefore lower the reactivity. For the complex **C 21** with an additional H_2O_2 ligand, a corresponding transition state **TS 21** has not been optimized, because olefin attack at O3 leads to the dissociation of the hydrogen peroxide ligand. For the aqua complex **C 20**, the calculated activation energy for epoxidation increases to the comparably high value of 24.2 kcal/mol.

The coordination of a strong donor ligand inhibits the molybdenum-catalyzed epoxidation of olefins. This was already reported by Mimoun et al.[23] However, the reason for the inhibition is a lower electrophilicity of the complex rather than the blocking of a free coordination site for the olefin by the strong donor ligands at the metal center. It is interesting to note the slight influence that coordination of an aqua ligand to methyloxodiperoxorhenium(VII) compounds has on the reactivity of olefin epoxidation. Moreover, Kühn, Rösch, and co-workers[50] have recently found that Re-catalyzed olefin epoxidation is accelerated in the presence of N ligands. From the results of this section, an important conclusion for Mo-catalyzed epoxidations can be drawn. Due to the coordination of the oxidant, such as H_2O_2 or *t*BuOOH, to the metal center and due to the high activation barriers for the stabilized complexes, these catalytic processes must involve different species formed in subsequent reaction steps. Thiel and co-workers recently gave experimental[13] and theoretical[17] evidence for a potential proton transfer from an alkyl hydroperoxide ligand ROOH that is coordinated to the metal center, to an η^2-peroxo group of [$MoO(\eta^2\text{-}O_2)_2(NH_3)(ROOH)$]. During intramolecular proton transfer, the metalladioxirane moiety $M(O_2)$ is opened and species of the type [$MoO(\eta^2\text{-}O_2)(\eta^1\text{-}OOH)(NH_3)(\eta^1\text{-}OOR)$] are formed. The proton-transfer step also seems to be possible from hydroperoxide coordinating to the metal center.[21] Hence, in the presence of hydrogen peroxide, additional reaction mechanisms have to be taken into account, as suggested by Sheldon,[1,51] Sharpless[52] and Thiel,[13] for metal-complex-catalyzed epoxidations with alkyl hydroperoxides.

Conclusions

The reactivity of Mimoun-type peroxo complexes used for the epoxidation of olefins depends on six degrees of freedom of our extended model system [$MOL(O_2)(OER_3)L'$] and CH_2CHR' in the following way (see Scheme 3):

Table 7. Calculated (B3LYP/III+//B3LYP/II) stabilization energies E_s [kcal/mol] for the addition of L′ = {□, H_2O, H_2O_2} to [$MoO(O_2)(O_2)(OPR_3)$] and activation energies E_a [kcal/mol] for ethylene epoxidation with [$MoO(O_2)(O_2)(OPR_3)L'$]; ZPE-corrected (B3LYP/II) values are given in parentheses

No.	(i) M	(ii) L	(iii) E	(iv) R	(v) R′	(vi) L′	E_s	E_a
2	Mo	O_2	P	CH_3 [a]	H	□	–	16.9 (17.9)
20	Mo	O_2	P	CH_3 [a]	H	H_2O	−11.6 (−8.6)	23.8 (24.2)
21	Mo	O_2	P	CH_3 [a]	H	H_2O_2	−15.0 (−12.6)	–[b]

[a] For geometry optimizations and frequency calculations, basis set STO-3G was used at the methyl groups. – [b] The H_2O_2 ligand is removed from the metal center during olefin attack.

(i) Metal M = Cr, Mo, W: In the complexes $[MO(O_2)_2(OER_3)]$, we find the trend in the epoxidation activity to be W > Mo > Cr. While atomic partial charges and thermodynamic considerations fail to predict activation energies, Charge Decomposition Analysis (CDA) of the transition states was employed as a powerful tool to reveal the relationship between reactivity and the electrophilicity at the metalladioxirane moieties.

(ii) Diperoxo versus monoperoxo compounds; L = O_2, O: Activity O_2 > O. The monoperoxotungsten complex apparently is an active oxidant, whereas the corresponding monoperoxomolybdenum species seems to be inactive.

(iii) Pnicogen E = N, P, As: Activity P > N, As. In agreement with experimental data, complexes with the weaker donor phosphane oxide are more electrophilic and, thus more active under homogeneous conditions than their N and As counterparts. However, the better extracting ability of the latter compounds makes them superior in a biphasic protocol.

(iv) Substituents at the pnicogen R = H, CH_3, C_2H_5: Activity H > CH_3, C_2H_5. Long alkyl chains at the pnicogen oxides used as ligands in the biphasic catalytic system (BASF) have no influence on reactivity, but adjust the Nernst equilibrium, thereby favoring quantitative extraction of the catalyst.

(v) Substituents at the olefin R′ = H, CH_3, CF_3, CH=CH_2, C_6H_5: Reactivity CH_3, CH=CH_2, C_6H_5 > H > CF_3. Due to the electrophilic nature of oxygen transfer, more nucleophilic olefins react faster. The epoxidation of π-conjugated olefins is highly asynchronous; the C−O bond at the terminal carbon atom is formed first.

(vi) Additional ligands at the metal center L′ = □ (free coordination site), H_2O: Activity □ > H_2O. The reason why donor ligands, such as H_2O, inhibit oxygen transfer from the molybdenum compounds is the lower electrophilicity at the peroxo functionalities, rather than blocking the free coordination site for the activation of the olefin. Complexes of the type $[MoO(O_2)_2(OPR_3)L']$, with proton-containing ligands L′, such as H_2O and H_2O_2, can be expected to form compounds with η^1-OOH ligands via proton transfer. These species are probably more reactive than η^2-peroxo complexes.

Acknowledgments

Dirk V. Deubel thanks Jan Frunzke for helpful discussions. He thanks the Fonds der Chemischen Industrie for a Kekulé Scholarship and the Deutscher Akademischer Austauschdienst for a NATO Fellowship. This work has also been supported by the Deutsche Forschungsgemeinschaft (SFB 260 and Schwerpunktprogramm Peroxidchemie). Excellent service has been provided by the computer center of the Philipps-Universität Marburg. Additional computer resources were granted by the HLRS Stuttgart.

[1] R. A. Sheldon, in *Applied Homogeneous Catalysis with Organometallic Compounds* (Eds.: B. Cornils, W. A. Herrmann), VCH, Weinheim, **1996**, vol. 1, p. 441.
[2] J. Koller, US *3.350.422*, **1967**; *US 3.351.635*, **1967**.
[3] [3a] A. Butler, M.-J. Clague, G. Meister, *Chem. Rev.* **1994**, 94, 625 and references cited therein. − [3b] V. Conte, F. Di Furia, S. Moro, *J. Mol. Catal.* **1997**, *120*, 93.
[4] [4a] I. V. Kozhevnikov, *Chem. Rev.* **1998**, *98*, 171. − [4b] C. Venturello, R. D′Aloisio, J. C. J. Bart, M. Ricci, *J. Mol. Catal.* **1985**, *32*, 107. − [4c] Y. Ishii, M. Ogawa, in *Reviews on Heteroatom Chemistry* (Eds.: A. Ohno, N. Furukawa), MYU, Tokyo, **1990**, vol. 3, p. 121; [4d] R. Neumann, M. Cohen, *Angew. Chem.* **1997**, *109*, 1810; *Angew. Chem. Int. Eg. Engl.* **1997**, *36*, 1738. − [4e] M. Bösing, A. Nöh, I. Loose, B. Krebs, *J. Am. Chem. Soc.* **1998**, *120*, 7252.
[5] M. H. Dickman, M. T. Pope, *Chem. Rev.* **1994**, *94*, 569.
[6] [6a] C. C. Romão, F. E. Kühn, W. A. Herrmann, *Chem. Rev.* **1997**, *97*, 3197 and references cited therein. − [6b] W. Adam, C. M. Mitchell, *Eur. J. Org. Chem.* **1999**, 785. − [6c] W. A. Herrmann, D. W. Marz, W. Wagner, J. G. Kuchler, G. Weichselbaumer, R. W. Fischer (Hoechst AG), *DE 3.902.357*, **1989**; *EP 90101439.9*, **1990**.
[7] [7a] A. M. Al-Aljouni, J. H. Espenson, *J. Am. Chem. Soc.* **1995**, *117*, 9243. − [7b] A. M. Al-Aljouni, J. H. Espenson, *J. Org. Chem.* **1996**, *61*, 3969. − [7c] H. Tan, J. H. Espenson, *Inorg. Chem.* **1998**, *37*, 467.
[8] K. Weissermel, H.-J. Arpe, *Industrial Organic Chemistry*, Wiley-VCH, New York, **1997**.
[9] [9a] H. Mimoun, *Angew. Chem.* **1982**, *94*, 750; *Angew. Chem. Int. Ed. Engl.* **1982**, *21*, 734. − [9b] H. Mimoun, I. Seree de Roch, L. Sajus, *Bull. Soc. Chem. Fr.* **1969**, 1481.
[10] G. Wahl, D. Kleinhenz, A. Schorm, J. Sundermeyer, R. Stowasser, C. Rummey, G. Bringmann, C. Fickert, W. Kiefer, *Chem. Eur. J.* **1999**, *5*, 3237.
[11] [11a] M. Schulz, J. H. Teles, J. Sundermeyer, G. Wahl (BASF AG) *DE 195.33.331.4*, **1995**. − [11b] M. Schulz, J. H. Teles, J. Sundermeyer, G. Wahl (BASF AG) *WO 10054*, **1995**.
[12] E. P. Talsi, K. V. Shalyaev, K. I. Zamaraev, *J. Mol. Catal.* **1993**, *83*, 347 and references cited therein.
[13] [13a] W. R. Thiel, T. Priermeyer, *Angew. Chem.* **1995**, *107*, 1870; *Angew. Chem. Int. Ed. Engl.* **1995**, *16*, 1737. − [13b] W. R. Thiel, *Chem. Ber.* **1996**, *129*, 575. − [13c] W. R. Thiel, *J. Mol. Catal. A* **1997**, *117*, 449. − [13d] W. R. Thiel, J. Eppinger, *Chem. Eur. J.* **1997**, *3*, 696.
[14] P. Gisdakis, S. Antonczak, S. Köstlmeier, W. A. Herrmann, W. A.; N. Rösch, *Angew. Chem.* **1998**, *110*, 2333; *Angew. Chem. Int. Ed.* **1998**, *37*, 2211.
[15] I. V. Yudanov, P. Gisdakis, C. Di Valentin, N. Rösch, *Eur. J. Inorg. Chem.* **1999**, *5*, 3603.
[16] D. V. Deubel, J. Sundermeyer, G. Frenking, *J. Am. Chem. Soc.* **2000**, *122*, 10101.
[17] A. Hroch, G. Gemmecker, W. R. Thiel, *Eur. J. Inorg. Chem.* **2000**, 1107.
[18] I. V. Yudanov, C. Di Valentin, P. Gisdakis, N. Rösch, *J. Mol. Catal.* **2000**, *158*, 189.
[19] C. Di Valentin, P. Gisdakis, I. V. Yudanov, N. Rösch, *J. Org. Chem.* **2000**, *65*, 2996.
[20] D. V. Deubel, G. Frenking, H. M. Senn, J. Sundermeyer, *Chem. Commun.* **2000**, 2469.
[21] D. V. Deubel, J. Sundermeyer, G. Frenking, *Org. Lett.*, **2001**, *3*, 329.
[22] J. Sundermeyer, *Angew. Chem.* **1993**, *105*, 1195; *Angew. Chem. Int. Ed. Engl.* **1993**, *32*, 1144.
[23] H. Mimoun, I. Seree de Roch, L. Sajus, *Tetrahedron* **1970**, *26*, 37.
[24] D. V. Deubel, J. Sundermeyer, G. Frenking, *Inorg. Chem.* **2000**, *39*, 2314.
[25] K. B. Sharpless, J. M. Townsend, D. R. Williams, *J. Am. Chem. Soc.* **1972**, *94*, 295.
[26] In Figure 5, the optimized structure of the model complex $[MoO(O_2)_2(OPH_3)]$ **R 10** is shown. Atom O2 is denoted *cis*, atom O3 is denoted *trans*. The activation energy for the transfer of the *cis*-oxygen atom was theoretically predicted to be 9.5 kcal/mol larger than for the *trans*-oxygen atom (ref.[16]).
[27] S. Dapprich, G. Frenking, *J. Phys. Chem.* **1995**, *99*, 9352.
[28] A. D. Becke, *J. Chem. Phys.* **1993**, *98*, 5648.
[29] P. J. Hay, W. R. Wadt, *J. Chem. Phys.* **1985**, *82*, 299.

[30] [30a] J. S. Binkley, J. A. Pople, W. J. Hehre, *J. Am. Chem. Soc.* **1980**, *102*, 939. – [30b] W. J. Hehre, R. Ditchfield, J. A. Pople, *J. Chem. Phys.* **1972**, *56*, 2257.
[31] G. Frenking, I. Antes, M. Böhme, S. Dapprich, A. W. Ehlers, V. Jonas, A. Neuhaus, M. Otto, R. Stegmann, A. Veldkamp, S. F. Vyboishchikov, *Reviews in Computational Chemistry* (Eds.: K. B. Lipkowitz, D. B. Boyd), VCH, New York, **1996**, vol. 8, p. 63.
[32] A. W. Ehlers, M. Böhme, S. Dapprich, A. Gobbi, A. Höllwarth, V. Jonas, K. F. Köhler, R. Stegmann, A. Veldkamp, G. Frenking, *Chem. Phys. Lett.* **1993**, *208*, 111.
[33] T. Clark, J. Chandrasekhar, G. W. Spitznagel, P. v. R. Schleyer, *J. Comput. Chem.* **1983**, *4*, 294.
[34] D. V. Deubel, G. Frenking, *J. Am. Chem. Soc.* **1999**, *121*, 2021.
[35] A. E. Reed, L. A. Curtiss, F. Weinhold, *Chem. Rev.* **1988**, *88*, 899.
[36] M. J. Frisch, G. W. Trucks, H. B. Schlegel, G. E. Scuseria, M. A. Robb, J. R. Cheeseman, V. G. Zakrzewski, J. A. Montgomery, Jr., R. E. Stratmann, J. C. Burant, S. Dapprich, J. M. Millam, A. D. Daniels, K. N. Kudin, M. C. Strain, O. Farkas, J. Tomasi, V. Barone, M. Cossi, R. Cammi, B. Mennucci, C. Pomelli, C. Adamo, S. Clifford, J. Ochterski, G. A. Petersson, P. Y. Ayala, Q. Cui, K. Morokuma, D. K. Malick, A. D. Rabuck, K. Raghavachari, J. B. Foresman, J. Cioslowski, J. V. Ortiz, B. B. Stefanov, G. Liu, A. Liashenko, P. Piskorz, I. Komaromi, R. Gomperts, R. L. Martin, D. J. Fox, T. Keith, M. A. Al-Laham, C. Y. Peng, A. Nanayakkara, C. Gonzalez, M. Challacombe, P. M. W. Gill, B. Johnson, W. Chen, M. W. Wong, J. L. Andres, C. Gonzalez, M. Head-Gordon, E. S. Replogle, and J. A. Pople, *Gaussian 98, Revision A.3*, Gaussian, Inc., Pittsburgh PA, **1998**.
[37] [37a] J. S. Dewar, *Bull. Soc. Chim. Fr.* **1951**, *18*, c71. – [37b] J. Chatt, L. A. Duncanson, *J. Chem. Soc.* **1953**, 2939.
[38] CDA 2.1, S. Dapprich, G. Frenking, Marburg, **1994**. The program is available via ftp.chemie.uni-marburg.de/pub/cda
[39] F. Jensen, *Introduction to Computational Chemistry*, Wiley, Chichester, **1999**.
[40] Note that these compounds $[MO(O_2)_2(NH_3)]$ are unsuitable models for the BASF system: A complex with an olefin directly bound to the metal center was not found as a minimum on the potential-energy surface with the $[MO(O_2)_2(NH_3)]$ model (ref.[19]) but with the $[MO(O_2)_2(OPR_3)]$ model (ref.[16]).
[41] [41a] R. Herges, *Angew. Chem.* **1994**, *106*, 261. – [41b] R. Herges, *J. Chem. Inf. Comput. Sci.* **1994**, *34*, 91.
[42] R. D. Bach, M. N. Glukhovtsev, C. Canepa, *J. Am. Chem. Soc.* **1998**, *120*, 775.
[43] G. Amato, A. Arcoria, F. P. Ballistreri, G. A. Tomaselli, *J. Mol. Catal.* **1986**, *37*, 165.
[44] [44a] G. Wahl, PhD thesis, Würzburg University, Germany, **1998**. – [44b] D. Kleinhenz, PhD thesis, Marburg University, Germany, **2000**.
[45] Utilizing the STO-3G basis set instead of 6−31G* at the methyl moieties for geometry optimization and frequency calculation provides results of the subsequent total-energy calculation at the B3LYP/III+ level without loss of accuracy (see Table 5).
[46] [46a] M. A. Barteau, R. J. Madix, *The Chemical Physics of Solid Surfaces and Heterogenious Catalysis* (Eds.: D. A. King, D. P. Woodruff), Elsevier, Amsterdam, **1982**, p. 95. – [46b] R. A. Van Santen, H. P. C. E. Kuipers, *Adv. Catal.* **1987**, *35*, 265. – [46c] W. M. H. Satchler, C. Backx, R. A. Van Santen, *Catal. Rev.* **1981**, *23*, 127.
[47] I. Fleming in *Frontier Orbitals and Organic Chemical Reactions*, Wiley, New York, **1976**.
[48] Note that experimental free-enthalpy values might differ from the calculated energies. For instance, the coordination of an additional ligand L′ to the metal center is an isokinetic reaction, i.e. the entropic contribution to the free enthalpy partially compensates the enthalpic stabilization. Solvation effects were not explicitly taken into account in our study because the molecules are too large. Furthermore, there is a basis-set-superposition error (BSSE), which is, however, expected to be very small since diffuse basis functions have been employed for energy calculations.
[49] In a previous study (ref.[24]), two isomers of the complex $[MoO(O_2)_2(OPH_3)(H_2O)]$ were found on the potential-energy surface. The OPH_3 and H_2O ligands occupy one equatorial and one axial coordination site of a pentagonal bipyramid. The isomer with the stronger phoshane oxide ligand in the equatorial position is favored by 5.3 kcal/mol over the isomer with the aqua ligand in the equatorial position. Due to electronic and steric reasons, we expected an even larger preference of the former isomer when the improved model $OPMe_3$ is utilized and omitted the investigation of the latter isomer using the improved model.
[50] F. E. Kühn, A. M. Santos, P. W. Roesky, E. Herdtweck, S. Scherer, P. Gisdakis, I. V. Yudanov, C. Di Valentin, N. Rösch, *Chem. Eur. J.* **1999**, *5*, 3603.
[51] R. A. Sheldon, *Recl. Trav. Chim. Pays-Bas* **1973**, *253*, 367.
[52] A. O. Chong, K. B. Sharpless, *J. Org. Chem.* **1977**, *42*, 1587.

Received October 14, 2000
[I00427]